Int. J. Nano Dimens., 12 (4): 402-410, Autumn 2021

ORIGINAL ARTICLE

Optical properties and surface growth mechanism of amorphous Carbon nanolayers

Elham Mohagheghpour[1], Marjan Rajabi*[,2], Reza Gholamipour[2], Sakineh Hosseinabadi[3]

[1]Radiation Applications Research School, Nuclear Sciences and Technology Research Institute, 14395836, Tehran, Iran

[2]Department of Advanced Materials and Renewable Energy, Iranian Research Organization for Science and Technology (IROST), 33535111, Tehran, Iran

[3]Department of Physics, East Tehran Branch, Islamic Azad University, Tehran, Iran

Received 15 April 2021, revised 01 August 2021, accepted 05 August 2021, available online 05 August 2021

Abstract

In this article, the growth kinetic and optical property of amorphous carbon (a-C) nanolayers deposited by ion beam sputtering deposition technique on glass substrates are investigated. The atomic force microscopy is used to measure the variation of surface roughness versus deposition time. According to the calculations, the roughness of thin films increases during the growth process as a fractal scaling law. The Hurst exponent (α) has a value higher than 0.5, and the growth exponent (β) changes in the range of 0.02 to 0.22. These fractal exponents predict that the growth process of amorphous carbon nanolayers obeys the rules of the Wolf-Villain model belonging to the Edwards-Wilkinson universality class, in which the relaxation and surface diffusion happen during the growth process. The results indicate that the optical band gap decreases by reducing the surface roughness, Hurst exponent and the correlation length during thin film growth which is the first observation of this trend.

Keywords: *Amorphous Carbon; Ion Beam Sputtering Deposition; Surface Growth Mechanism; Thin Film; Wolf-Villain Model.*

How to cite this article

Mohagheghpour E, Rajabi M, Gholamipour R, Hosseinabadi S. Optical properties and surface growth mechanism of amorphous Carbon nanolayers. Int. J. Nano Dimens., 2021; 12(4): 402-410.

INTRODUCTION

A surface is the first interface of a thin film that is in contact with other materials, and the surface roughness is a crucial point in determining the physical properties of thin films, especially in industrial applications [1]. For example, the fabrication of efficient sensors (gas, light, and biosensors) needs a high active surface area, or the real area of contact between materials affects the heat transfer between the solids [2]. The active surface area is proportional to roughness parameters such as standard deviation (which indicates the vertical grain size), roughness or Hurst exponent, and correlation length (that specifies the lateral grain size) [3]. Due to the importance of the roughness parameters, their influence on the electrical, optical, and mechanical properties of different materials has been investigated through experimental and theoretical methods [4-8].

The amorphous carbon (a-C) is a wide bandgap semiconductor with valuable properties such as tunable bandgap, optical transparency in the visible and IR regions, high mechanical hardness, high electrical resistivity, and chemical inertness [9-13]. Due to these properties, amorphous carbon thin films have been used widely in optics, mechanical engineering, and material science. Ultrathin carbon films are used as a protective coating in the magnetic storage industry, as electrodes for corrosion sensors at high temperatures and overcoats in food (for packaging) and medical (implants) industries [4, 13, 14]. According to investigations, the surface roughness of a-C films, which is an influential parameter in determining the optical properties and magnetic storage

* Corresponding Author Email: *mrajabi@irost.ir*

density, depends on growth techniques, substrate condition (materials and temperature) and film composition (sp^2 and sp^3 content) [14].

There are some discrete statistical models such as the ballistic deposition (BD) model [15-18], Eden model [18], solid on solid (SOS) model [19], and Wolf-Villain [20-22] model that explain the behavior of atoms during the growth process and surface evolution. The Wolf- Villain model was used by I. Koponen et al. to describe the roughening of amorphous carbon surfaces due to ion bombardment [21]. Their Monte Carlo investigations indicated that the bombarded surfaces had self-affine topography. There are several growth models for the deposition of amorphous carbon films. The preferential displacement of sp^2 bonded atoms and relaxation by thermal spikes are the basis of most of these models [23, 24]. There are also some molecular simulations on the first stages of tetrahedral amorphous carbon (ta-C) growth, but they focus only on the sp^3 evolution [25]. Casiraghi et al. used Monte Carlo simulations to investigate the smoothing effects caused by thermal spikes in ultrathin amorphous carbon films and defined a growth mechanism for the ta-C [14].

Due to the importance of atomic processes occurring during the a-C film deposition for determining its density as well as optical, mechanical, and electrical properties, in this article, we have investigated the relations that may exist between optical properties and surface roughness. The growth kinetics of the amorphous carbon thin films deposited by the ion beam sputtering deposition technique with fixed ion energy at room temperature on glass substrates is described by calculating the fractal exponents.

EXPERIMENTAL PROCEDURE

The amorphous carbon thin films were deposited on glass substrates with the dimensions of 1.5 ×1.5 cm^2 and the surface roughness of 1.31 ± 0.73 nm using the ion beam sputtering deposition (IBSD) technique. Before the deposition process, the substrates were cleaned by using acetone and ethanol in an ultrasonic bath, respectively. The carbon source was a high purity graphite plate (12 ×15 cm^2). The base pressure in the deposition chamber was about 1-2×10^{-5} Torr. During the deposition process, the chamber pressure was kept steady at 3-6×10^{-5} Torr. Also, the substrate temperature was kept constant at room temperature. The voltage of the accelerator and the ion current were 2200V and 25 mA, respectively. The deposition time (5, 10, 15, and 20 min) was a growth variable parameter, while the other parameters were kept constant. After each process, the samples were cooled down to room temperature in an argon-filled atmosphere.

The layer thickness was determined by doing reflection interference measurements (AvaSpec-2048) and using AvaSoft - Thin Film software. The surface topography of the glass substrate and a-C thin films were characterized by using the atomic force microscope (AFM; DME- DS 95) working in a tapping mode with the scan rate of approximately 3 Hz with a typical scan area of 1×1 μm^2 (256 points in each x and y-axis). The optical properties of thin films included transmission and reflectance spectra, were examined by UV/visible spectrophotometer (Cary500 and AvaSpec-2048). The Raman spectra were measured by using the 532 nm excitation wavelength of the Nd-YAG laser with the power of 1 mW.

Fractal analysis

During the growth process of thin films, the surface roughness can be defined by the root mean square of height as follows [22]:

$$W = \left(\left(h - \bar{h} \right)^2 \right)^{1/2} \quad (1)$$

where $\bar{h}$ is an average of height values in a given area and < > indicates the averaging over different samples. Generally, the roughness evolution during surface growth can be described by the Family-Vicsek fractal scaling law as [22]:

$$W\left(L;t\right) \sim L^{\alpha} f\left(t / L^{\alpha/\beta}\right) \quad (2)$$

where L is the size of the sample, *t* is the growth time, β is called the growth exponent, and α ($0 \le \alpha \le 1$) is the roughness or the Hurst exponent. There are two different scaling regimes depending on parameter $u \equiv t / L^{\alpha/\beta}$: for short times, i.e., $u \ll 1$, $W \sim t^{\beta}$, and, for $u \gg 1$, $f\left(u\right) = constant.$

In addition to the growth exponent and Hurst exponent, a correlation function describes the surface morphology. The correlation function is defined as:

$$C\left(s\right) = \left[h\left(\vec{r}\right) - \bar{h} \right] \left[h\left(\vec{r}^{\,'}\right) - \bar{h} \right] \quad (3)$$

where $s = \left| \vec{r} - \vec{r}' \right|$. The correlation length, l_{cor},

determines the length over which the correlation function reaches 1/*e* of its maximum value.

The exponents α and β uniquely characterize the self-affine geometry of the surface and its dynamics during the growth process. Their values determine the universality class of various growth mechanisms. For example, in the random deposition (RD) model, α is undefined and $\beta = 0.5$. There is no correlation between two neighboring sites, and the particles stick where they fall. The random deposition with surface diffusion belongs to Edward-Wilkinson (EW) universality class. In this model, the particles do not stick to the surface immediately; they relax and diffuse to find the site with a lower height. In the one-dimensional type of this model, the roughness and growth exponents are 0.5 and 0.25, respectively. Therefore, one could describe the type of experimental growth process using discrete models, which are simulated according to the given growth rules that govern the physical features of growth phenomena. Specifying scaling exponents, including the growth and roughness exponents, can determine the kinetic roughening and the universality class in which each growth model is located. There are various discrete models which describe the mechanism of growth process, such as stochastic modeling of MBE and diffusion considering models [23, 26-30], conservative restricted solid on solid (CRSOS) [31, 32], Wolf-Villain (WV), and the Das Sarma–Tamborenea (DT) models [22, 33], in which surface diffusion and relaxation take place. For example, it has been found that the growth and roughness exponents are $\beta = 0.20 \pm 0.020$ and $\alpha = 0.66 \pm 0.03$ for the Wolf-Villain model [34-37]. In the present study, by calculating the roughness and the growth exponent of a-C thin films deposited by the IBSD technique, we determined the dynamics and growth mechanism of the mentioned rough surfaces during the growth process. Furthermore, we predicted the model by which the growth occurred in addition to its universality class.

RESULTS AND DISCUSSION

Fig. 1 shows a typical XRD spectrum of the a-C nanolayer deposited on the glass substrate. As can be seen, the spectrum does not have a peak in the larg range, so the structure of the deposited layers on the glass substrate is amorphous.

Fig. 2 shows a typical Raman spectrum of the thickest a-C nanolayer deposited on the glass substrate (the low power of laser restricted the Raman measurement of layers with smaller thickness). This spectrum consists of two broad peaks at around 1552cm^{-1} and 1398 cm^{-1}, labeled as peaks G and D, respectively. Both peaks are related to sp^2 sites. The G peak is due to the band stretching in aromatic (rings) and olefinic (chains) of sp^2 molecules, and peak D is a breathing mode of sp^2 rings [1]. This mode is not observed in perfect graphite and only appears in the presence of the disorder and its intensity is strictly connected to the presence of a sixfold aromatic ring [1, 19, 22]. The Raman spectrum was deconvoluted using the Lorentzian function to determine the values of the I_D/I_G ratio, the D and G peak position, and FWHM of a- C nanolayer, as listed in Table 1.

If the FWHM of the D band is more than 50 cm^{-1}, the intensity ratio of the D band to G band (I_D/I_G) will be related to the size of the graphite

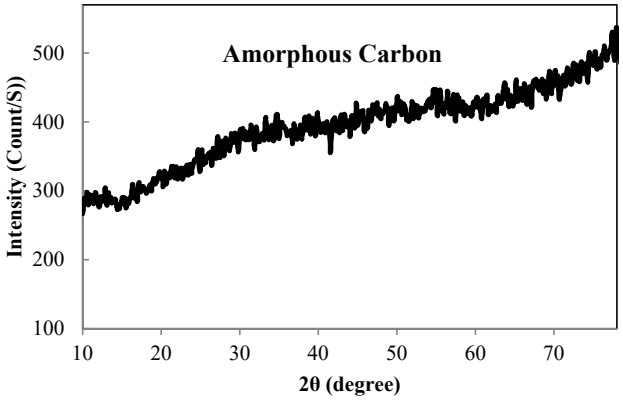

Fig. 1. XRD spectra of a-C film deposited on glass substrates.

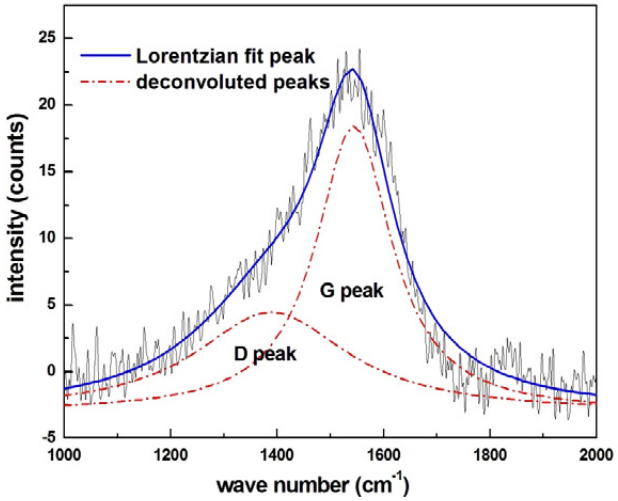

Fig. 2. Raman spectrum of a-C film deposited on glass substrates. The film thickness is approximately equal to 70 nm.

Table 1. Data extracted from the Raman spectrum of a-C thin film (thickness ~ 70 nm) by Lorentzian deconvolution.

Band	Intensity	FWHM (cm^{-1})	Peak position (cm^{-1})
D	7.53	345.97	1398.2
G	21.58	172.33	1544.5

Table 2. The relation between the kinetic growth exponents and the optical properties of thin films with different thicknesses.

Code	Time (min)	Thickness (nm)	Roughness (nm)	Hurst exponent (α)	$l_{cor}(\mu m)$	E_{Tauc} (eV)
T5	5	32	2.56±0.50	0.73±0.05	0.14±0.03	3.40
T10	10	37	8.26±0.95	0.68±0.05	0.10±0.03	3.10
T15	15	56	1.06±0.18	0.59±0.05	0.08±0.03	2.63
T20	20	70	0.87±0.24	0.57±0.05	0.07±0.03	2.62

cluster (L_a) as follows [11]:

$$\frac{I_D}{I_G} = cL_a^2 \qquad (4)$$

where c is equal to ~0.0055 and L_a is in Angstrom [11]. The intensity ratio of the current spectrum is calculated to be ~ 0.35. Thus, the mean size of graphite crystallites is found to be ~8 Å at a thickness of ~70 nm.

The transmittance and reflectance spectra of the amorphous carbon nanolayers are shown in Fig. 3(a) and Fig. 3(b), respectively. As illustrated in Table 2, the thickness of nanolayers changes from 32 to 70 nm by increasing the deposition time. As depicted in Fig. 3(c), at the specific wavelength of 550 nm, the transmittance of these films was reduced by the enhancement of film thickness. At the same time, the reflectance had no particular behavior. As expected, the highest transmittance belonged to the nanolayer with a lower thickness of ~32 nm.

The optical bandgap energy of nanolayers was estimated by using the Tauc method [38]. The absorption coefficient α, near the band edge varied with the photon energy, $h\vartheta$, according to the following equation [11, 38]:

$$\alpha = B\left(h\vartheta - E_{opt}\right)^n / h\vartheta \qquad (5)$$

where *B* is a constant, *h* is the Planck constant, E_{opt} is the optical bandgap energy, ϑ is the frequency, and n is a number characterizing the transition process. Due to the indirect nature of electron transitions in a-C and its amorphous

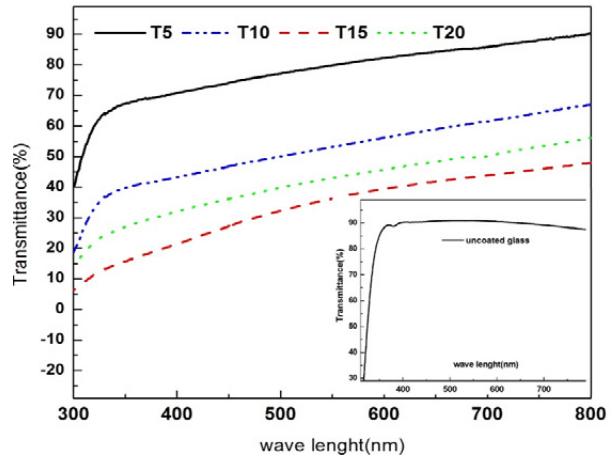

(a)

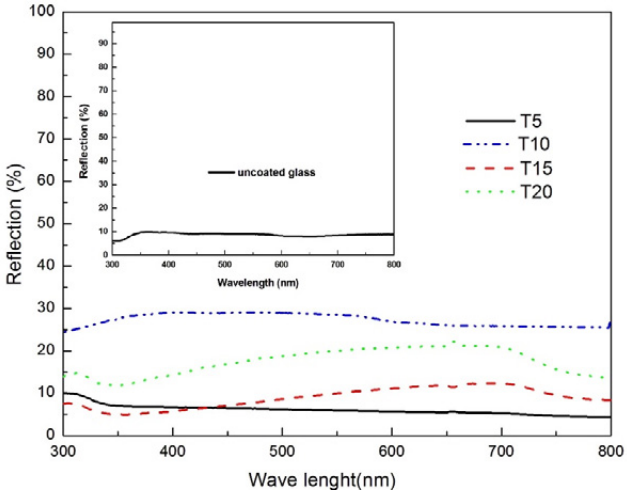

(b)

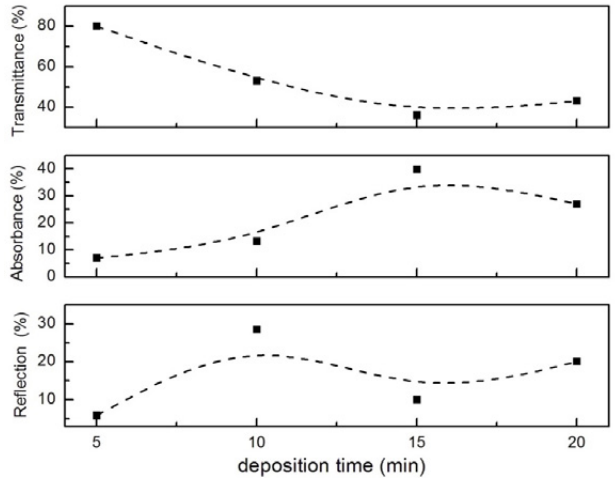

(c)

Fig. 3. (a) Transmittance (incet: Transmittance of uncoated glass) (b) Reflectance (incet: Reflectance of uncoated glass) and (c) the specific value of transmission, absorption, and reflection at 550 nm versus the film thickness.

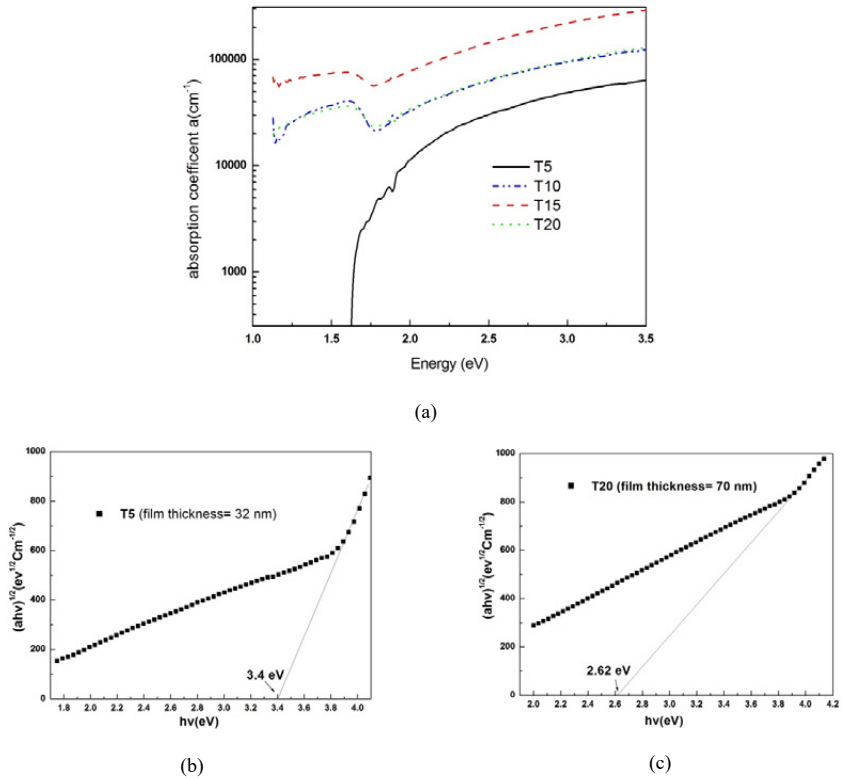

Fig. 4. (a) The absorption coefficients of a-C films. (b) and (c) the estimation of the optical bandgap of a-C thin films by Tauc relation.

nature, the parameter of n in the Tauc equation is considered equal to 2 [39]. The absorption coefficient is calculated by using the following equation:

$$\alpha = ln\left[\left(1-R\right)^2 / T\right] / d \qquad (6)$$

where R and T are, respectively, the reflection and transmission coefficients and d is the film thickness. The optical bandgap value is determined by extrapolating the linear part of $(\alpha h\vartheta)^{\frac{1}{2}}$ versus $h\vartheta$ (Figs. 4(a), 4(b) and 4(c)). The intercept of the plot with the horizontal axis determines the optical gap energy of a-C thin films, which change in the range of 3.40 eV to 2.62 eV by changing film thickness, as listed in Table 2. According to these data, the bandgap broadening happens with the reduction of film thickness in nanolayers. Such expansions could be the result of the quantum confinement effect or broadening of the localized tail states. The optical properties of a-C films are usually discussed in terms of transitions between the occupied π states to unoccupied π^* states (associated with sp^2) because the σ and σ^* states (associated with sp^3) are further separated from each other. Moreover, the overall optical bandgap of the films is the average of the local band gaps of different clusters. Thus, the bigger clusters have smaller bandgaps [38, 40]. Since the optical bandgap of the deposited films reduces with the increase in the film thickness and the mean size of graphite crystallites is found to be 8 Å at the thickness of 70 nm (according to Equation 4), it can be predicted that the average size of the graphite cluster and I_D/I_G ratio in the samples with the lower thickness is lower than 8 Å and 0.35, respectively, because the optical bandgap reduces with the increase in the film thickness.

Figs. (5(a), 5(b), 5(c) and 5(d)), indicate AFM topography images of a-C nanolayers deposited on glass substrates. The corresponding roughness values are present in Table 2. As mentioned previously, the substrate roughness is 1.31 ± 0.73 nm. Thus, at the first stage of deposition, the values of roughness increase because the accumulation of carbon atoms at the top of the hills is faster than the valleys on the substrate surface. However, with the continuation of the

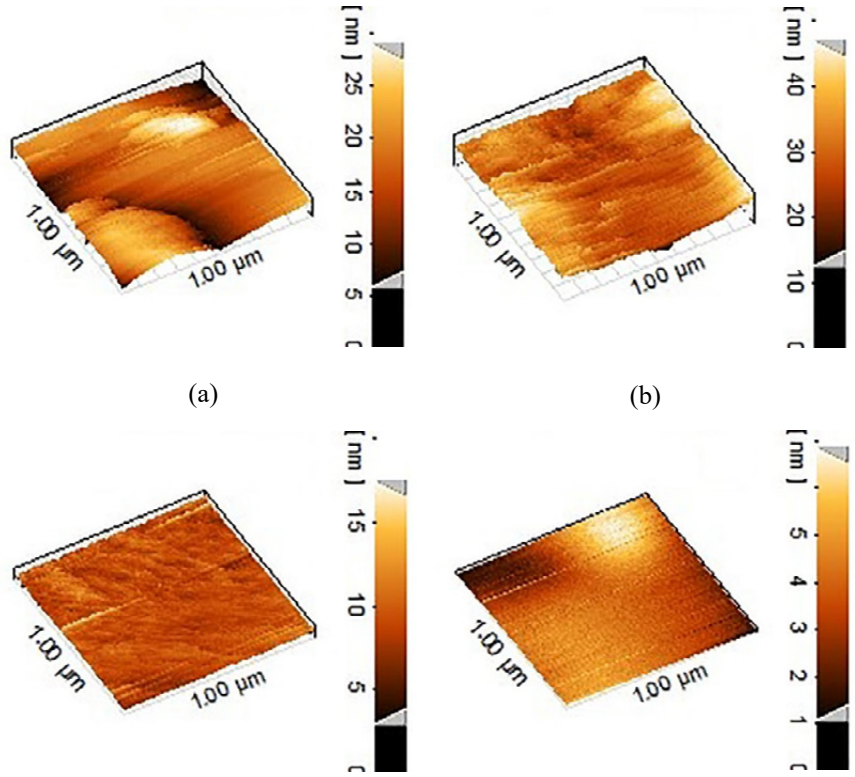

Fig. 5. AFM images of the a-C films prepared with different thicknesses (a) T5, (b) T10, (c) T15, and (d) T20.

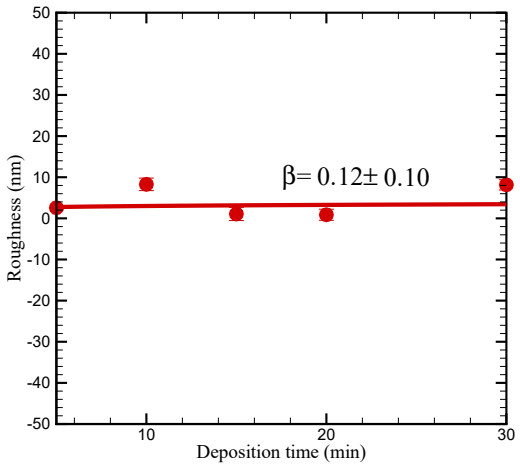

Fig. 6: Roughness evolution as a function of thickness.

deposition, the filling of the valleys leads to the reduction of surface roughness [41].

The Hurst or roughness exponent (α) and the correlation length (l_{cor}) extracted from AFM measurements are listed in Table 2. The values of the Hurst exponent were calculated from the multi-fractal detrended fluctuation analysis (MFDFA) method [42]. Fundamentally, in the presence of random walk or uncorrelated noise, the Hurst exponent is equal to 0.5, and the surface is isotropic and self-similar [22]. In this research, the values of the Hurst exponent are higher than 0.5 (α>0.5), indicating the existence of long-range correlations in the height fluctuations of the nanolayers. Therefore, the relaxation process and surface diffusion occur during the growth process of amorphous carbon nanolayers on glass substrates by ion beam sputtering deposition technique.

Fig. 6 shows the diagram of roughness, *W*, against deposition time, *t*. In this figure, the power-fit relation of *W* against *t* is investigated, in which the growth exponent, β, in the relation $W \cong t^{\beta}$ is extracted as 0.12 ± 0.10 (0.02-0.22). The most relevant two-dimensional growth models with local surface diffusion have been done by Kotrla et al. and Das Sarma et al. [33, 43-45]. Kotrla et al. found that the two-dimensional generalization of the Wolf-Villain model had

exponent $\beta = 0.20 \pm 0.020$ and $\alpha = 0.66 \pm 0.03$ [36, 37]. Furthermore, the mentioned exponents are in good agreement with the results obtained by Lopez et al. and Šmilauer et al. [34, 35]. The values of β and α for the investigated a-C thin films corresponded to the Wolf-Villain model as indicated above. In the Wolf-Villain model, particles are added to random positions and diffuse to maximize their number of neighbors. Then, they choose the place with the strongest binding to the surface or the position with the largest number of neighbors. In this model, diffusion of atoms is relevant, and it belongs to the EW universality class [46]. Also, the value of $\beta \sim 0 - 0.1$ has been reported for Diamond-like carbon (DLC) films [14]. The correlation length has been calculated in a-C thin films with different thicknesses. Comparing the results of Table 2 indicates that the sample with the lowest thickness of 32 nm (T5) has the highest correlation length, and it is more correlated than the other samples.

In amorphous carbon thin films, the optical gap depends on the content and order of sp^2 sites which tend to form clusters. The sp^2 cluster size enhancement reduces the value of the optical gap [47]. The reduction of the optical bandgap in this research is accompanied by the increase of deposition time (film thickness) and the decrease of correlation length and Hurst exponent. Also, according to these results, the surface relaxation and diffusion process in amorphous carbon thin films deposited using the ion beam sputtering deposition technique can be described by the Wolf-Villain model. Thus, we may conclude that the diffusion process during deposition or modification of surfaces by using ion bombardment belongs to the EW universality class. Also, both deposited and modified coatings have self-similar topography.

CONCLUSION

In conclusion, we have investigated the relations between the optical properties and surface roughness of amorphous carbon thin films with different thicknesses deposited by the ion beam sputtering deposition technique. The results indicated that the bandgap energy was decreased by the reduction of the Hurst exponent. The growth exponent β was 0.02-0.22, and the Hurst exponents α were more than 0.5. So in this study, the growth mechanism of a-C thin film belonged to the discrete statistical Wolf-Villain model and the EW universality class. For the first time, we report that the statistical parameters change with the same trend of bandgap energy.

ACKNOWLEDGMENT

Dr. Elham Mohagheghpour wants to thank Mr. Yasser Amoosi for offering help in reviewing and revising the manuscript for grammar and syntax.

CONFLICT OF INTERESTS

There is no conflict of interest.

REFERENCES

[1] Lüth H. , (2001), Solid surfaces, interfaces and thin films. Springer Book.

[2] Persson B, Tosatti E., (2001), The effect of surface roughness on the adhesion of elastic solids. *The J. Chem. Phys.* 115: 5597-610.

[3] Vahabi M., Jafari G., Mansour N., Karimzadeh R., Zamiranvari J., (2008), Stochastic features of rough surfaces: Analysis of laser-induced silicon surface modification. *J. Statistic. Mech: Theory and Exp.* 2008: P03002.

[4] Ciavarella M., Joe J., Papangelo A., Barber J., (2019), The role of adhesion in contact mechanics. *J. Royal Soc. Interf.* 16: 20180738.

[5] Timoshevskii V., Ke Y., Guo H., Gall D., (2008), The influence of surface roughness on electrical conductance of thin Cu films: An ab initio study. *J. Appl. Phys.* 103: 113705-113709.

[6] Persson B. N., Albohr O., Tartaglino U., Volokitin A., Tosatti E., (2004), On the nature of surface roughness with application to contact mechanics, sealing, rubber friction and adhesion. *J. Physics: Condens. Matt.* 17: R1-R62.

[7] Kubiak K., Wilson M., Mathia T., Carval P., (2011), Wettability versus roughness of engineering surfaces. *Wear.* 271: 523-528.

[8] Javidjam A., Hekmatshoar M. H., Hedayatifar L., Abad S. N. K., (2018), Effect of surface roughness on electrical conductivity and hardness of silver plated copper. *Mat. Res. Express.* 6: 036407-036411.

[9] Lv Y., Zhou Y., Liu J., Shao M., Zhang Z., Song G., (2020), Production and performance study of Diamond-Like Carbon resistive electrode in MPGD. *Nucl. Instrum. Meth. A.* 958: 162759-162766.

[10] Gasab M. T. I., Uchiyama M., Nakatani T., Valanezhad A., Watanabe I., Fujiyama H., (2016), Advanced DLC coating technique on silicone-based tubular medical devices. *Surf. Coat. Technol.* 307: 1084-1087.

[11] Robertson J., (2002), Diamond-like amorphous carbon. *Mater. Sci. Eng: R: Reports.* 37: 129-281.

[12] Tang Y., Li Y., Yang Q., Hirose A., (2011), Characterization of hydrogenated amorphous carbon thin films by end-Hall ion beam deposition. *Appl. Surf. Sci.* 257: 4699-4705.

[13] Chiang K., Yang L., Wei R., Coulter K., (2008), Development of diamond-like carbon-coated electrodes for corrosion sensor applications at high temperatures. *Thin Solid Films.* 517: 1120-1124.

[14] Casiraghi C., Ferrari A., Ohr R., Chu D., Robertson J., (2004), Surface properties of ultra-thin tetrahedral amorphous carbon films for magnetic storage technology. *Diam. Related Mater.* 13: 1416-1421.

[15] Braun G., (2020), On the growth of a ballistic deposition

model on finite Graphs. *arXiv Preprint arXiv:200109836.*
[16] Grüner C., Grüner S., Mayr S. G., Rauschenbach B., (2020), Avoiding anisotropies in on-lattice simulations of ballistic deposition. *Phys. Status Solidi (b).* 2020: 2000036.
[17] Alves S. G., Ferreira S. C., (2016), Scaling, cumulant ratios, and height distribution of ballistic deposition in 3+ 1 and 4+ 1 dimensions. *Phys. Rev. E.* 93: 052131-052131.
[18] Alves S. G., Ferreira S. C., (2012), Eden clusters in three dimensions and the kardar-parisi-zhang universality class. *J. Stat. Mech: Theor. Expt.* P10011.
[19] Hosseinabadi S., Masoudi A. A., Sadegh Movahed M., (2010), Solid-on-solid model for surface growth in 2+1 dimensions. *Phys. B.* 405: 2072–2077.
[20] Chen Y., Tang G., Xun Z., Zhu L., Zhang Z., (2017), Schramm–loewner evolution theory of the asymptotic behaviors of (2+ 1)-dimensional Wolf–Villain model. *Phys. A: Statist. Mech. Appl.* 465: 613-620.
[21] Koponen I., Hautala M., Sievänen O-P., (1997), Simulations of self-affine roughening and ripple formation on ion bombarded amorphous carbon surfaces. *Nucl. Instrum. Meth. B.*129: 349-355.
[22] Barabási A-L., Stanley H. E., (1995), Fractal concepts in surface growth: Cambridge University Press. 388 pages · ISBN-10: 0521483182.
[23] To T. B., de Sousa V. B., Reis F. D. A., (2018), Thin film growth models with long surface diffusion lengths. *Phys. A: Statist. Mech. Appl.* 511: 240-250.
[24] Pang E., Vo N., Philippe T., Voorhees P., (2015), Modeling interface-controlled phase trans formation kinetics in thin films. *J. Appl. Phys.* 117: 175304-175309.
[25] Casiraghi C., Ferrari A., Robertson J., (2005), The smoothness of tetrahedral amorphous carbon. *Diam. Related Mater.* 14: 913-920.
[26] Sarakinos K., (2019), A review on morphological evolution of thin metal films on weakly-interacting substrates. *Thin Solid Films.* 688: 137312-137316.
[27] Luis E. E. M., de Assis T. A., Ferreira S. C., Andrade R. F., (2019), Local roughness exponent in the nonlinear molecular-beam-epitaxy universality class in one dimension. *Phys. Rev. E.* 99: 022801-022805.
[28] Reis F. A., (2013), Normal dynamic scaling in the class of the nonlinear molecular-beam-epitaxy equation. *Phys. Rev. E.* 88: 022128-022133.
[29] Oliveira F. A., Ferreira R., Lapas L. C., Vainstein M. H., (2019), Anomalous diffusion: A basic mechanism for the evolution of inhomogeneous systems. *Frontiers in Phys.* 7: 18-25.
[30] Sturrock M., (2016), Stochastic reaction–diffusion algorithms for macromolecular crowding. *Phys. Biol.* 13: 036010-036015.
[31] Dae H. K., Jin Min K., (2011), Conserved noise restricted-solid-on-solid model on fractal substrates. *Phys. Rev. E.* 84: 011105-011110.
[32] Park S-C., Kim D., Park J-M., (2001), Derivation of continuum stochastic equations for discrete growth models. *Phys. Rev. E.* 65: 015102-015107.
[33] Huang Z-F., Gu B-L., (1996), Growth equations for the Wolf-Villain and Das Sarma-Tamborenea models of molecular-beam epitaxy. *Phys. Rev. E.* 54: 5935-5941.
[34] Chame A., Reis F. A., (2004), Scaling of local interface width of statistical growth models. *Surf. Sci.* 553: 145-154.
[35] Zhipeng X., Gang T., Kui H., Hui X., Dapeng H., Yan Li., (2012), Asymptotic dynamic scaling behavior of the (1+1)-dimensional Wolf-Villain model. *Phys. Rev. E.* 85: 041126-041131.
[36] Zhipeng X., Gang T., Kui H., Hui X., Dapeng H., Yuling C., Rongji W., (2010), Mound morphology of the 2+1 -dimensional Wolf–Villain model caused by the step-edge diffusion effect. *Phys. A: Statis. Mech. Appl.* 389: 245635-245644.
[37] Kotrla M., Levi A., Šmilauer P., (1992), Roughness and nonlinearities in (2+1)-dimensional growth models with diffusion. *EPL (Europhysics Letters).* 20: 25-31.
[38] Sánchez-Vergara M. E., Alonso-Huitron J. C., Rodriguez-Gómez A., Reider-Burstin J. N., (2012), Determination of the optical GAP in thin films of amorphous dilithium phthalocyanine using the tauc and cody models. *Molecules*. 17: 10000-10013.
[39] Mohagheghpour E., Rajabi M., Gholamipour R., Larijani M. M., Sheibani S., (2016), Correlation study of structural, optical and electrical properties of amorphous carbon thin films prepared by ion beam sputtering deposition technique. *Appl. Surf. Sci.* 360: 52-58.
[40] Sagar R. U. R., Zhang X., Xiong C., Yu Y., (2014), Semiconducting amorphous carbon thin films for transparent conducting electrodes. *Carbon*. 76: 64-70.
[41] Salvadori M., Martins D., Cattani M., (2006), DLC coating roughness as a function of film thickness. *Surf. Coat. Technol.* 200: 5119-5122.
[42] Hosseinabadi S., Rajabpour M., Movahed M. S., Allaei S. V., (2012), Geometrical exponents of contour loops on synthetic multifractal rough surfaces: Multiplicative hierarchical cascade p model. *Phys. Rev. E.* 85: 031113-031117.
[43] Lai Z-W., Sarma S. D., (1991), Kinetic growth with surface relaxation: Continuum versus atomistic models. *Phys. Rev. Lett.* 66: 2348-2352.
[44] Sarma S. D., Ghaisas S., (1992), Solid-on-solid rules and models for nonequilibrium growth in 2+ 1 dimensions. *Phys. Rev. Lett.* 69: 3762-3768.
[45] Villain J., (1991), Continuum models of crystal growth from atomic beams with and without desorption. *J. Phys. I.* 1: 19-42.
[46] Hosseinabadi S., Karimi Z., Masoudi A. A., (2020), Random deposition with surface relaxation model accompanied by long-range correlated noise. *Phys. A.* 560: 125130-125135.
[47] Baydoğan N. D., (2004), Evaluation of optical properties of the amorphous carbon film on fused silica. *Mater. Sci. Eng. B.* 107: 70-77.